Simulation Study of Surveillance Strategies for Faster Detection of Novel SARS-CoV-2 Variants

Selina Patel, Fergus Cumming, Carl Mayers, André Charlett,[1] Steven Riley[1]

Earlier global detection of novel SARS-CoV-2 variants gives governments more time to respond. However, few countries can implement timely national surveillance, resulting in gaps in monitoring. The United Kingdom implemented large-scale community and hospital surveillance, but experience suggests it might be faster to detect new variants through testing arrivals in England for surveillance. We developed simulations of emergence and importation of novel variants with a range of infection hospitalization rates to the United Kingdom. We compared time taken to detect the variant though testing arrivals at borders in England, hospital admissions, and the general community. We found that sampling 10%–50% of arrivals at borders in England could confer a speed advantage of 3.5–6 weeks over existing community surveillance and 1.5–5 weeks (depending on infection hospitalization rates) over hospital testing. Directing limited global capacity for surveillance to highly connected ports could speed up global detection of novel SARS-CoV-2 variants.

In the current phase of the COVID-19 pandemic, waves of SARS-CoV-2 infection are driven by novel variants and their sublineages, which continue to cause illness and death with potential to disrupt society. Government policies to mitigate those effects are more effective if they are put in place early but have substantial associated costs and therefore should not be implemented unless necessary. Evaluating the threat of an emergent variant to determine a proportionate response requires time to gather evidence. Global surveillance of SARS-CoV-2 and other respiratory pathogen genome sequences aims to contribute to the rapid detection of novel variants so that countries have more time to make policy decisions to respond. However, few countries have the capacity and resources for timely national surveillance, resulting in gaps in international monitoring.

During the first few years of the pandemic, Hong Kong implemented a strict traveler quarantine protocol (*1*). Travelers underwent testing for SARS-CoV-2 infection during their quarantine, and 10% of detected imported infections were sequenced. Retrospective sequence data from those travelers reflects the global emergence and spread of variants over time. In some instances, traveler-based testing in Hong Kong detected variant circulation in other nations before it had been domestically sequenced and uploaded to GISAID (https://www.gisaid.org). The Hong Kong border screening experience suggests opportunities for traveler-based surveillance to speed up detection of novel variants and compensate for internationally incomplete coverage of domestic genomic surveillance.

To pilot this approach, the United States sampled arrival flights from countries with a high travel volume (India, South Africa, Nigeria, Brazil, France, United Kingdom, Germany) for voluntary surveillance testing (*2*). During November 2021–January 2022, the United States achieved a 10% response rate and detected Omicron BA.2 seven days earlier and Omicron BA.3 forty-three days earlier than anywhere else in the country.

In the United Kingdom, although traveler-based surveillance was not used when border measures were decreased in 2022, previous traveler-based testing policies required inbound passengers to undergo testing shortly after arrival (*3*). The United Kingdom also conducted a large community survey of SARS-CoV-2 surveillance, and all patients experiencing symptomatic respiratory disease in hospital undergo testing for SARS-CoV-2 infection (*4*). Although

Author affiliations: University College London, London, UK (S. Patel); UK Health Security Agency, London (S. Patel, F. Cumming, C. Mayers, A. Charlett, S. Riley); Imperial College London, London (S. Riley)

DOI: https://doi.org/10.3201/eid2911.230492

[1]These senior authors contributed equally to this article.

reporting times were variable across those testing routes, Omicron was isolated and detected in England from a mandatory day 2 border test in an inbound traveler on November 16, 2021 (*5*). This test was 5 days earlier than a non–travel-associated sample that was obtained on November 21. Moreover, most of the earliest samples of Delta during the first 2 weeks of detection in the United Kingdom were also collected from travelers, despite the availability of universal testing in the community alongside surveillance at that time (*6*). To explore the potential utility of border screening for more rapid detection of variants, we simulated the time to obtaining a sample of an imported novel variant for genomic sequencing through sampling arrivals at ports in England, compared with existing large-scale community surveillance and testing of persons who came to a hospital.

Methods

Variants in our scenarios are considered to be imported from a country of a similar level of connectedness as between England and China. Over the most recent winter (December 2022–January 2023), China showed a huge increase in transmission of SARS-CoV-2 and resulting deaths after lifting of regulations that were part of previous Zero-COVID policy (*7*). This transmission risks the emergence of novel variants that could have a major effect on the epidemiology of COVID-19 elsewhere in the world. We replicated simulations for 4 scenarios of imported novel variants with infection hospitalization rates (IHRs) of 1.0%, 1.5%, 2.0%, and 2.5%. During the initial spread of the Alpha variant, the IHR was estimated at 1.0%–2.0%, which caused major impact and resulted in the reintroduction of national lockdown laws to mitigate its spread (*8*,*9*).

We generated a single-wave epidemic curve originating in an area with a total population of 60 million. The index case occurred on day 0. A Poisson distribution with a mean of 2 was assumed as the offspring distribution (i.e., each case, on average, transmits an infection to 2 other persons). The distribution of the generation time (the interval between the infection in a primary case and the infection in a secondary case caused by a transmission from the primary case) was assumed to be a gamma distribution with a shape parameter of 7 and a scale parameter of 1 Thus, the effective reproduction number was 2, and the average doubling time was 7 days. The offspring distribution for the first 2 generations was fixed at exactly 2. We assumed that the epidemic increased unchecked for 16 weeks, after which the mean of the offspring distribution was reduced to represent both control countermeasures and depletion of susceptible persons in the population. Between the 17th and 26th generations, we reduced the mean by 0.1 at each successive generation, such that the reproduction number was 1 at the 26th generation. From the 27th generation onward, the mean of the offspring distribution was reduced at each generation by 0.01786 (1/56).

The incubation period for each generated infection was drawn from the published pooled lognormal distribution in McAloon et al. (*10*). This procedure provides an estimated mean of 1.63 and SD of 0.5 for a normal distribution of the logged incubation period distribution. Published estimates of the infectious period before and after symptom onset are extremely heterogeneous, as described in Byrne et al. (*11*). Thus, the presymptomatic infectious period was fixed at 2 days, and the combined presymptom and postsymptom infectious period for each generated infection was drawn from a normal distribution with a mean of 10 days and an SD of 1.33 days. This procedure provides a relatively small probability of being infectious 10 days after symptom onset, as reported by Singanayagam et al. (*12*). We rounded those 2 periods to an integer, providing the duration for disease. Daily prevalence as estimated by combining the simulated cases over their duration for all days after the day the index case occurred. In the simulations, the period postinfectiousness in which PCRs could still detect virus was ignored. The simulated epidemic curve was truncated at 300 days.

We obtained the number of incoming travelers on each day that were incubating or infectious by using a draw from a binomial distribution. We assumed that the number of daily travelers was fixed at 250 and a probability equal to the origin areas prevalence on that day (i.e., assuming that persons infected are as equally likely to travel as persons not infected).

For detection at the border, conditional on the simulations having $\geq$1 infected traveler, we selected a representative sample ranging from 10% to 50% of travelers for testing. We further assumed that the percentage who are in an infectious state (detectable) was 73%, the sensitivity of the test 85%, and the percentage of positive test results, 50%. We used those percentages as the probability of draws from independent Bernoulli distributions; a detection was declared if each of those draws were 1.

We assumed growth in the destination country to be the same as growth in the origin area. Incubating or infectious incursions were drawn from a Bernoulli distribution with a probability of 73%. The time remaining in these states was obtained from a uniform distribution and the mean of the offspring distribution

modified to account for this time. We assumed that travelers would spend all of their infectious period in the destination country. Daily incidence and prevalence of cases in the destination country were generated, but with the destination country population being assumed to be 56 million. We simulated 1,000 destination country epidemics.

For detection of a simulated case in the hospital setting, we assumed IHRs of 1.0%–2.5% and allocated simulated cases to presence in a hospital by using a draw from a Bernoulli distribution with a probability of 1%. We assumed that time to seeking care at a hospital because of infection followed a gamma distribution with a shape parameter of 1.4 and a scale parameter of 4 (i.e., giving a mean of 5.6 days, but with substantial variation). The percentage of persons seeking care who were tested was 50%; sensitivity of the test and percentage of positive test results sequenced were set as previously stated. Simulations were applied to each of the 1,000 destination country epidemics.

For detection of a simulated case in a community setting, we used a range of community cohort surveillance sizes from 20,000 (≈0.04% of the population) to 200,000 (≈0.36% of the population). We assumed that each person in this surveillance was tested every 2 weeks. We applied simulations to each of the 1,000 destination country epidemics The number detected each day obtained from a draw from a binomial distribution by using the number tested each day and the simulated daily prevalence, combined with the sensitivity of the test and the percentage of positive test results.

The time to detecting a case from border, hospital, and community testing has been summarized by using the empirical 5th, 25th, 50th, 75th, and 95th percentiles of the simulation sets. We ran simulations using Stata version 17.0 (StataCorp LLC, https://www.stata.com). For all simulation sets, we used a unique random number seed in a 64-bit Mersenne Twister pseudo-random number generator (default pseudo-random number generator in Stata). A detailed technical description of the methods used is available (https://wwwnc.cdc.gov/EID/article/29/11/23-0492-App1.pdf).

Results

First, we simulated the time to detection of an imported novel variant through different sampling fractions (10%, 20%, 30%, 40%, and 50%) of traveler arrivals in England. We assumed that the prevalence of infection in the passenger population was equal to that of the epidemic curve generated for the country of origin over time (Appendix 1). In our scenarios, there was a nonlinear relationship between increasing sampling fraction and decreasing days to detection starting from 131 days to detection through sampling 10% of passenger arrivals (Table 1). The greatest reduction in time to detection was gained between sampling fractions 10%–20%, which led to a median 8-day decrease in time to detection. Thereafter, the time gained began to decrease with increasing sampling fraction.

Next, we simulated the time to detection through testing 50% of persons coming to a hospital in England. We assumed that growth in incidence in England (the destination country) was the same as that in the country of origin. We ran simulations for scenarios where variants had IHRs of 1.0%, 1.5%, 2.0%, and 2.5%. Although time to detection in hospitals decreased with increasing IHR, in all 4 scenarios it took >10 days longer to detect a novel variant in hospitals than by sampling 10%–50% of travelers arriving in England (Table 2).

Finally, we simulated the earliest time to obtaining a sample of an imported novel variant through testing a community cohort sampled for surveillance. We ran scenarios implementing a sample size of 0.04% (20,000) to 0.36% (200,000) of the population in England, assuming the same growth in prevalence in the population over time as that assumed for incidence. Increasing the size of the community cohort from 0.04% to 0.36% of the population decreased the time to detection by 3 weeks (175 days reduced to 154 days) (Table 3). For the sample size of existing community surveillance in England, which comprises ≈140,000 tests every 2 weeks, the simulated earliest time to detection was 157 days.

We found that, for border testing, the range of the median time to detection from the index case was 131 days (10% of travelers tested) to 114 days (50% of travelers tested). This result compares with 150

Table 1. Simulated time to detect a novel variant since index case in study of traveler testing for surveillance of novel SARS-CoV-2 variants

	Empirical percentiles of simulated time to detection distribution, d				
Percentage tested	5th	25th	Median	75th	95th
10	104	121	131	140	150
20	96	114	123	131	141
30	94	110	119	126	136
40	89	107	115	123	131
50	86	105	114	121	130

Table 2. Simulated time to detect a novel variant since index case through hospital testing in study of traveler testing for surveillance of novel SARS-CoV-2 variants

Infection hospitalization rate (%)	Empirical percentiles of simulated time to detection distribution, d				
	5th	25th	Median	75th	95th
0.01 (1)	124	141	150	157	167
0.015 (1.5)	122	138	147	154	162
0.02 (2)	117	134	143	151	159
0.025 (2.5)	115	132	142	149	159

days (1% IHR) to 142 days (2.5% IHR) for the median of the earliest time to detection in hospitals, assuming 50% of persons seeking care are tested. Also, we found medians of 175 days (testing a cohort of 0.04% of the population) versus 154 days (testing a cohort of 0.36% of the population) for the earliest time to detection through community surveillance. Detailed study results are provided (https://wwwnc.cdc.gov/EID/article/29/11/23-0492-App2.pdf).

Discussion

Our simulations indicate that sampling a relatively small percentage, 10%, of inbound travelers for surveillance could reduce the time to detection of the first case of an imported novel variant of SARS-CoV-2 in the England by 26 days compared with existing community surveillance. Increasing sampling fraction of travelers to 50% could increase this speed advantage to 43 days. Depending on IHR (1.0%–2.5%), sampling 10% of inbound travelers would also detect a variant 11–19 days faster than testing hospital admissions for surveillance. However, sampling 50% of arrivals would lead to detection 4–5 weeks faster than hospital testing.

Our simulated results appear concordant with the closest available observed data. In the United States, testing 10% of passengers on arrival flights from countries with a high travel volume resulted in Omicron BA.2 being detected 7 days earlier and Omicron BA.3 being detected 43 days earlier than anywhere else in the country (2). In comparison with our scenarios, a 10% sampling fraction resulted in detection of a novel variant 1.5–4 weeks sooner than in other settings. However, the extent to which further comparisons can be drawn between our results and this experience is limited. The scale of community and healthcare surveillance in the United States is much smaller than is assumed in our scenarios, and, unlike in our scenarios, US arrivals were required to present a negative test result before departure. In addition, the time between specimen collection and reporting sequence data can be extremely variable between testing pathways, which makes it challenging to observe the speed advantage gained in this example through sampling strategy alone.

Our findings are also broadly in agreement with more distantly related retrospective data from community testing and policies such as managed quarantine services (MQS) and requirement to test on or shortly after arrival in a country. Testing inbound travelers has detected or collected some of the earliest samples of imported novel variants nationally and globally, even during periods when universal testing has been available in the community. In Hong Kong,

Table 3. Simulated time to detect a novel variant since index case through community testing in study of traveler testing for surveillance of novel SARS-CoV-2 variants

Community testing cohort size (% destination country population)	Time to detection (days since emergence of index case), summaries from 1,000 simulations				
	5th percentile	25th percentile	Median	75th percentile	95th percentile
20,000 (0.04)	145	165	175	183	191
30,000 (0.05)	144	161	170	178	187
40,000 (0.07)	140	158	168	176	185
50,000 (0.09)	138.5	156	166	175	184
60,000 (0.11)	137	155.5	165	172	182
70,000 (0.13)	137	154	163	171	181
80,000 (0.14)	136	153	162	170	179
90,000 (0.16)	133	151	161	169	177
100,000 (0.18)	133.5	150.5	160	168	178
110,000 (0.20)	130	150	159	167	176
120,000 (0.21)	130	148	158	166.5	176
130,000 (0.23)	130.5	149	158	165	174
140,000 (0.25)	129	148	157	164	173
150,000 (0.27)	129	146	156	163	172
160,000 (0.29)	127.5	146	155.5	163	172
170,000 (0.30)	127	146	155	164	173
180.000 (0.32)	126	145	154	162	171
190,000 (0.34)	128	145	154	162	173
200,000 (0.36)	127	144.5	154	162	171

sequence data were collected for 10% of all infections detected through MQS. Retrospective analysis of those records and external data sources indicate that traveler-based testing was either a good reflection, or an early indicator, of the global emergence and spread of novel variants. For example, Omicron (B1.1.529) was detected in Hong Kong through a sample obtained in an MQS on November 13, 2021 (*13*), which was uploaded to GISAID on November 23 (*13*). This upload triggered UK investigations on November 24, resulting in government intervention to delay further introduction and spread (*14*). Most of the earliest samples of Omicron subsequently collected in the United Kingdom were from persons who had recently traveled (*5*). Thus, Omicron samples collected through MQS in Hong Kong were able to be used as prospective evidence for policy decisions because of rapid genomic sequencing of samples and data reporting. In the United States, early samples of Omicron were also collected, frequently from persons who had a history of recent travel. However, long lag times from data collection to reporting indicated that this factor was not known until December 1, 2021 (*15*).

We also report that sampling 50% of persons seeking care at hospitals for surveillance in our scenarios detected a novel variant with an IHR of 2.5% ≈8 days faster than a variant with an IHR of 1.0%. A lower IHR could either be caused by less severe disease associated with the variant or the availability of effective COVID-19 therapies preventing severe outcomes. An increased number of persons seeking care at hospitals when IHR is greater reduces the speed advantage gained through traveler-based surveillance. However, waves of infection caused by variants that have higher IHRs are more likely to be detected earlier in the country of emergence as a result of increasing hospital visits. This factor often already offers governments outside the country of emergence some advanced warning of the impact of a new wave of infection associated with greater illness and death, despite gaps in global genomic surveillance. Therefore, the greatest potential impact of early detection through genomic surveillance might be for those variants that have an IHR large enough to cause societal disruption but low enough that it is slower to identify through hospital admissions.

To simulate the time to detection of an imported novel variant in England in each of our scenarios, we have made some simplifying assumptions. We have assumed that the prevalence of infection in air passengers is the same as that in the country of origin at the time of the departure of their flight, specimens are collected from a random sample of passengers, and the variant doubling time in the destination country is the same as that of in country of origin once seeded. A lower reproductive rate across both countries would have extended the time to detection of a novel variant across all surveillance strategies. However, a lower reproductive rate in only the destination country would have increased the speed advantage of border surveillance testing strategies.

We have also considered only direct incursions from the country of emergence of a novel variant to the destination country. We have not considered the effect of indirect incursions linked to infected travelers arriving from other countries where transmission might also be occurring. This decision is a simplification of observed human behavior, population immunity profiles, and transmission dynamics. However, we do not expect that a model comprising more complex representations of those processes would result in greatly different overall conclusions. We have also not attempted to carry out an economic evaluation of each surveillance strategy. Although such an evaluation is a major factor in policy and public health decisions, it would require a detailed cost-effectiveness analysis that is beyond the scope of this study.

In this report, we have focused the results and discussion on simulated scenarios that compare border surveillance with existing surveillance in hospitals and the community in England and the United Kingdom. However, this surveillance in England achieved greater coverage than for most countries. Therefore, as routine testing and surveillance for SARS-CoV-2 is decreasing globally, this study probably provides conservative estimates of the potential speed advantage that could be gained through traveler-based surveillance approaches. Also, if there were concerns about a specific country at any point in time, temporary programs would be able to achieve high sample proportions at the border with only limited numbers of samples compared with other ongoing or potential global programs.

It is useful to recognize that the collection of a sample of a novel variant for detection is the first step to evaluate the threat of a novel variant. In our scenarios, we do not consider the time it takes to sequence and report data obtained from a sample. Sequencing and reporting times are extremely variable across countries which can greatly reduce the time gained through effective sampling approaches (*16*). In addition, a full threat assessment requires robust estimates of severe outcomes in addition to temporal and geospatial descriptions of variant epidemiology to inform policy decisions.

Global surveillance of SARS-CoV-2 genome sequences contributes to rapid detection of novel variants to give governments more time to respond. However, few countries have capacity to implement national surveillance with timely sequencing and reporting, resulting in major gaps in global coverage of surveillance. In our scenarios, directing limited global capacity for surveillance to the most highly connected ports could provide governments with much more time to respond to future novel variants of SARS-CoV-2 and their sublineages. Beyond informing national approaches to surveillance, this approach also underscores the potential usefulness of international collaboration to achieve high global coverage of surveillance and provide governments with more time to make policy decisions to respond to novel variants of SARS-CoV-2.

About the Author

Ms. Patel is a research scientist at University College London, London, UK, and a principal public health scientist at the UK Health Security Agency, London. Her primary research interests are public health, infectious diseases, and surveillance approaches.

References

1. Gu H, Cheng SS, Krishnan P, Ng DY, Chang LD, Liu GY, et al. Monitoring international travelers rriving in Hong Kong for genomic surveillance of SARS-CoV-2. Emerg Infect Dis. 2022;28:247–50. https://doi.org/10.3201/eid2801.211804
2. Wegrzyn RD, Appiah GD, Morfino R, Milford SR, Walker AT, Ernst ET, et al. Early detection of severe acute respiratory syndrome coronavirus 2 variants using traveler-based genomic surveillance at 4 US airports, September 2021–January 2022. Clin Infect Dis. 2023;76:e540–3. https://doi.org/10.1093/cid/ciac461
3. Williams GH, Llewelyn A, Brandao R, Chowdhary K, Hardisty KM, Loddo M. SARS-CoV-2 testing and sequencing for international arrivals reveals significant cross border transmission of high risk variants into the United Kingdom. EClinicalMedicine. 2021;38:101021. https://doi.org/10.1016/j.eclinm.2021.101021
4. Office of National Statistics. COVID-19 infection survey [cited 2022 Oct 3]. https://www.ons.gov.uk/surveys/informationforhouseholdsandindividuals/householdandindividualsurveys/covid19infectionsurvey
5. UK Health Security Agency. SARS-CoV-2 variants of concern and variants under investigation in England. Technical briefing 32. Report no. 32 [cited 2023 Sep 29]. https://assets.publishing.service.gov.uk/government/uploads/system/uploads/attachment_data/file/1060337/Technical-Briefing-38-11March2022.pdf
6. Public Health England. SARS-CoV-2 variants of concern and variants under investigation in England. Technical briefing 14. Report no. 14 [cited 2023 Sep 29]. https://www.gov.uk/government/publications/investigation-of-novel-sars-cov-2-variant-variant-of-concern-20201201
7. Reuters. China reports 59,938 COVID-related hospital deaths since Dec. 8. January 14, 2023 [cited 2023 Jan 16]. https://www.reuters.com/world/china/china-reports-59938-covid-related-hospital-deaths-since-dec-8-2023-01-14
8. Public Health England. SARS-CoV-2 variants of concern and variants under investigation in England. Technical briefing 13. Report no. 13 [cited 2023 Sep 2]. https://assets.publishing.service.gov.uk/government/uploads/system/uploads/attachment_data/file/990339/Variants_of_Concern_VOC_Technical_Briefing_13_England.pdf
9. Baker C, Kirk-Wade E, Brown J, Barber S. Coronavirus: a history of English lockdown laws. July 1, 2023 [cited 2023 Jan 7]. https://commonslibrary.parliament.uk/research-briefings/cbp-9068
10. McAloon C, Collins Á, Hunt K, Barber A, Byrne AW, Butler F, et al. Incubation period of COVID-19: a rapid systematic review and meta-analysis of observational research. BMJ Open. 2020;10:e039652. https://doi.org/10.1136/bmjopen-2020-039652
11. Byrne AW, McEvoy D, Collins AB, Hunt K, Casey M, Barber A, et al. Inferred duration of infectious period of SARS-CoV-2: rapid scoping review and analysis of available evidence for asymptomatic and symptomatic COVID-19 cases. BMJ Open. 2020;10:e039856. https://doi.org/10.1136/bmjopen-2020-039856
12. Singanayagam A, Patel M, Charlett A, Lopez Bernal J, Saliba V, Ellis J, et al. Duration of infectiousness and correlation with RT-PCR cycle threshold values in cases of COVID-19, England, January to May 2020. Euro Surveill. 2020;25:2001483. https://doi.org/10.2807/1560-7917.ES.2020.25.32.2001483
13. Gu H, Krishnan P, Ng DY, Chang LD, Liu GY, Cheng SS, et al. Probable transmission of SARS-CoV-2 Omicron variant in quarantine hotel, Hong Kong, China, November 2021. Emerg Infect Dis. 2022;28:460–2. https://doi.org/10.3201/eid2802.212422
14. UK Health Security Agency. SARS-CoV-2 variants of concern and variants under investigation in England. Technical briefing 29. Report no. 29 [cited 2023 Sep 29]. https://assets.publishing.service.gov.uk/government/uploads/system/uploads/attachment_data/file/1036501/Technical_Briefing_29_published_26_November_2021.pdf
15. CDC COVID-19 Response Team. SARS-CoV-2 B.1.1.529 (Omicron) variant—United States, December 1-8, 2021. MMWR Morb Mortal Wkly Rep. 2021;70:1731–4. https://doi.org/10.15585/mmwr.mm7050e1
16. Brito AF, Semenova E, Dudas G, Hassler GW, Kalinich CC, Kraemer MU, et al.; Swiss SARS-CoV-2 Sequencing Consortium. Global disparities in SARS-CoV-2 genomic surveillance. Nat Commun. 2022;13:7003. https://doi.org/10.1038/s41467-022-33713-y

Address for correspondence: Selina Patel, UK Health Security Agency, Nobel House, London SW1P 3HX, UK; email: selina.patel.17@ucl.ac.uk

Article DOI: https://doi.org/10.3201/eid2911.230492

Simulation Study of Surveillance Strategies for Faster Detection of Novel SARS-CoV-2 Variants

Appendix 1

Methods for earliest detection a novel variant by border testing, hospital, and community surveillance

Simulated epidemic at origin

A single occurrence of a novel variant occurs on day zero (d_0). To obtain the resultant epidemic curve, offspring, and generation time, distributions of $Poisson(2)$ and $\Gamma(7,1)$ were used respectively with the offspring fixed at 2 for the first 2 generations to ensure the epidemic establishes (Appendix 1 figure 1). Random draws of generation times were rounded to the nearest integer.

This choice of offspring and generation time provides an epidemic curve where R_0 is 2 with a doubling time of 7 days. The variant was assumed to grow unchecked for 16 generations, after which the mean of the offspring distribution was reduced by 0.1 of each successive generation to obtain an offspring distribution $Poisson(1)$ at the 26th generation, i.e., R_t of 1 after around 6 months. From the 27th generation onwards, the mean of the offspring distribution was reduced at each generation by 0.01786 (1/56).

Fifty-two generations were simulated, but a 300-day cut off used to ensure that chains with shorter than average generation times did not impact completeness of simulated infections, there being a probability of around 0.0002 of obtaining a sum of 52 draws from $round(\Gamma(7,1),1)$ being <300.

For each simulated infection k, the day of infection d_k was obtained by summation of the generation times for their predecessors. The incidence on day d is obtained by a summation over all n infections, $IO_d = \sum_{k=1}^{n}(d_k == d)$, where $(d_k == d)$ is 1 if d_k equals d, 0 otherwise. The simulated epidemic curve is shown in Appendix 1 Figure 2, for which the cumulative incidence up to day 300 since d_0 is around 23,000,000.

For each simulated infection, a log incubation period was obtained from a random draw from $N(1.63,0.5)$, with time of symptom onset occurring at $d_k^s = d_k + l_k$. The 10th, 50th, and 90th centiles for this incubation period distribution are ≈2.7, 5.1, and 9.7 days, respectively (Appendix 1 Figure 3) (*1*).

The infectious period distribution was assumed to be $N(10,1.33)$, with the period of infectiousness beginning 2 days before symptom onset. Thus, the first day of being infectious for the k^{th} infection occurs on day $d_k^s - 2$. If $d_k^s - 2 < d_k$ then l_k is set to 0, and if $d_k^s - 2 > 19$ then l_k is set to 19. Appendix 1 Figure 3 provides a visualization of the assumed incubation period distribution and the temporal probability of infectiousness (*2,3*).

The pre-infectious period (d_k to $d_k^s - 3$) and infectious period ($d_k^s - 2$ to $d_k^s - 2 + i_k$) are combined and the prevalence of being in either state on day d is obtained from $PO_d = \frac{1}{N_o}\sum_{k=1}^{n}\left(d_k \le d \le (d_k + l_k + i_k - 2)\right)$, where $d_k \le d \le (d_k + l_k + i_k - 2)$ is 1 if d is greater or equal to $d_k$and less than or equal to $d_k + l_k + i_k - 2$, 0 otherwise. The infection prevalence is shown in Appendix 1 Figure 4.

Simulated epidemics at destination

For each day from d_0 it is assumed for simplicity, that there are a fixed number of direct air travelers n_t departing the origin for the destination. These travelers are assumed to have the same infection prevalence as the origin on the day of departure and all flights depart and arrive on the same day. On day d the number of infected travelers is obtained from a random draw from $binomial(n_t, PO_d)$. A simulated infected traveler is in the infectious state if a random draw from $binomial(1, \pi_{inf})$ is equal to 1, otherwise they are in a pre-infectious state. For the simulated incursions in both the pre-infectious and infectious state, the time in their state has been reduced by multiplication with a random draw from a uniform distribution

$Uniform([0,1])$, and for those in the infectious state, their simulated number of offspring has similarly been reduced.

One thousand simulated incidence growth curves have been generated from the simulated incursions, for a total of 30 generations. For simplicity, it is assumed that the offspring distribution and generation time distribution are the same as at the origin. While this is likely to be true for the latter, for the former this would implicitly assume that population mixing in the origin and destination are similar. It has also been assumed that detection is only possible during the infectious state, and the post infectiousness period where PCR tests could still detect virus has been ignored. Thus, $ID_d = \sum_{k=1}^{n}(d_k^s == d)$, where $(d_k^s == d)$ is 1 if d_k^s equals d, 0 otherwise.

The incidence growth curves have been converted to disease prevalence growth curves by using the same methods previously described but ignoring the days in the pre-infectious state. These are shown in Appendix Figures 5 and 6.

The disease prevalence on day d is obtained from $PD_d = \frac{1}{N_D}\sum_{k=1}^{n}\left(d_k^s - 2 \le d \le (d_k^s - 2 + i_k)\right)$, where $d_k^s - 2 \le d \le (d_k^s - 2 + i_k)$ is 1 if d is greater or equal to $d_k^s - 2$ and less than or equal to $d_k^s - 2 + i_k$, 0 otherwise.

While for most simulations the growth of incident cases is modest, there are a small proportion where exceptional growth is observed. Because the objective was to gain an understanding of the earliest time to detection, no account has been taken of either depletion of those susceptible in the population or effective control measures both of which would cause the simulations with exceptional growth to turn over and decline. It has been assumed that such behavior would only occur post the earliest detections so are not a major consideration.

Time to earliest detection

For each of testing arrivals at the border, testing those sufficiently ill to present at a hospital, and testing those enrolled in community surveillance, simulations were implemented as outlined in future sections with one thousand such simulations performed for each. For all simulation sets, a unique random-number seed was used in a 64-bit Mersenne Twister pseudo-random-number generator.

The simulated earliest time of detection, i.e., earliest specimen date, ignoring any sample processing and reporting delays is obtained for each simulation with selected centiles of the simulated distributions of earliest detection times presented. For results in the paper, the median time to earliest detection is presented, with time in relation to the occurrence of the very first case d_0 being used throughout.

Time to earliest detection for testing at the border (T_b)

The number of incoming travelers n_d^I on each day that are either incubating or infectious is obtained by using a draw from $binomial(n_t, PO_d)$. For simplicity, an assumption that those traveling are independent of infection status has been made. Although this assumption will influence the time to earliest detection, which would occur later if prevalence in travelers is lower, it is unlikely to affect greatly any relative difference in the times to earliest detection at the border, or in either hospital or community surveillance.

The number of infected travelers being tested on day d, $n_d^{tested}$is obtained by using a draw from $binomial(n_d^I, \pi_t)$, provided n_d^I>0. The test on the k^{th} simulated infection is considered positive (b_k^+) if it is an infectious state, not having a false negative test, and being successfully sequenced. This was obtained by multiplying the random draws from three Bernoulli distributions, $binomial(1, \pi_{inf})$, $binomial(1, \pi_{sens})$, and $binomial(1, \pi_{seq})$, with a detection being declared if each of these draws are 1, otherwise considered a failure to detect. It has been assumed that the microbiological test has a sensitivity of 85%, and specificity of 100%, and that for technical reasons only 50% of positives isolates will lead to a sequence being successfully obtained.

For each detection at the border b_k^+, $d_k^{b^+}$is the day on which the positive specimen is taken. The time to earliest detection is $T_b = \min_{k \in \{b_k^+\}} d_k^{b^+}$.

Time to earliest detection for testing at hospitals (T_h)

From each of the 1000 simulated disease incidence growth curves in the destination country, the number of infections each day that would result in a hospital admission n_d^h was obtained from a random draw from $binomial(ID_d, \pi_{IHR})$, provided ID_d>0. The number of those hospitalized that will get tested, n_d^{ht} was obtained from a random draw from $binomial(n_d^h, \pi_h)$, provided n_d^h>0.

The k^{th} infected simulation is considered positive h_k^+ if it is not a false-negative test result and is successfully sequenced. This was obtained by multiplying random draws from two Bernoulli distributions, $binomial(1, \pi_{sens})$, and $binomial(1, \pi_{seq})$, with a detection being declared if each of both these draws are 1, otherwise considered a failure to detect.

For each hospital detection h_k^+, the day on which the positive specimen is taken $d_k^{h^+}$ was obtained from $d_k^s + t_h$, where d_k^s is the day of symptom onset of the k^{th} infection, and t_h is the time from symptom onset to hospitalization, taken as a random draw from a $\Gamma(5,2)$ and rounded to the nearest integer as shown in Appendix 1 Figure 7. The time to earliest detection is obtained by using $T_h = \min_{k \in \{h_k^+\}} d_k^{h^+}$.

Time to earliest detection for testing in the community (T_c)

It has been assumed that persons in community surveillance test every 2 weeks, and for simplicity the number of daily tests is $\frac{n_c}{14}$. From each of the 1000 simulated disease prevalence growth curves in the destination country, the number of simulated prevalent infections that would be tested on day d in community surveillance $n_d^{c^t}$ was obtained from a random draw from $binomial\left(round\left(\frac{n_c}{14}, 1\right), PD_d\right)$, provided PD_d>0.

The k^{th} infected simulation is considered positive c_k^+ if it is not a false negative test and is successfully sequenced. As before, this was obtained by multiplying random draws from two Bernoulli distributions, $binomial(1, \pi_{sens})$, and $binomial(1, \pi_{seq})$, with a detection being declared if each of these draws are 1, otherwise considered a failure to detect. For each detection in the community c_k^+, $d_k^{c^+}$ is the day on which the positive specimen is taken. The time to earliest detection is obtained by using $T_c = \min_{k \in \{c_k^+\}} d_k^{c^+}$.

References

1. McAloon C, Collins Á, Hunt K, Barber A, Byrne AW, Butler F, et al. Incubation period of COVID-19: a rapid systematic review and meta-analysis of observational research. BMJ Open. 2020;10:e039652. PubMed https://doi.org/10.1136/bmjopen-2020-039652

2. Byrne AW, McEvoy D, Collins AB, Hunt K, Casey M, Barber A, et al. Inferred duration of infectious period of SARS-CoV-2: rapid scoping review and analysis of available evidence for asymptomatic and symptomatic COVID-19 cases. BMJ Open. 2020;10:e039856. PubMed https://doi.org/10.1136/bmjopen-2020-039856

3. Singanayagam A, Patel M, Charlett A, Lopez Bernal J, Saliba V, Ellis J, et al. Duration of infectiousness and correlation with RT-PCR cycle threshold values in cases of COVID-19, England, January to May 2020. Euro Surveill. 2020;25:2001483. PubMed https://doi.org/10.2807/1560-7917.ES.2020.25.32.2001483

Appendix1 Table. Parameters used

	Symbol	Estimates/distributions used
Population of origin	N_O	60,000,000
Population of destination	N_D	56,000,000
Offspring	c_k	$\text{Poisson}(2)$
Generation time	g_k	$\text{round}(\Gamma(7,1),1)$
Incubation period	l_k	$\text{round}\left(e^{N(1.63,0.5)},1\right)$
Infectiousness period	i_k	$\text{round}(N(10,1.33),1)$
Day of infection for the k^{th} simulated infection	d_k	
Day of symptom onset for the k^{th} simulated infection	d_k^s	
Infection incidence in origin on day d	IO_d	
Disease incidence in destination on day d	ID_d	
Infection prevalence in origin on day d	PO_d	
Disease prevalence in destination on day d	PD_d	
Direct travelers per day	n_t	100, 250, 500
Proportion of travelers tested	π_a	0.01, 0.02, 0.05.0.10, 0.20
Probability infectious $\overline{i_k/(l_k+i_k-2)}$	π_{inf}	0.73
PCR Test sensitivity	π_{sens}	0.85
Positive successfully sequenced	π_{seq}	0.5
IHR	π_{IHR}	0.005,0.01,0.015,0.02,0.025
Proportion of hospital presentations testing	π_h	0.1, 0.2, 0.3, 0.4, 0.5
Time to hospital presentation	t_h	$\text{round}((\Gamma(5,2),1)$
Size of community surveillance	n_c	20,000–200,000 (steps of 10,000)

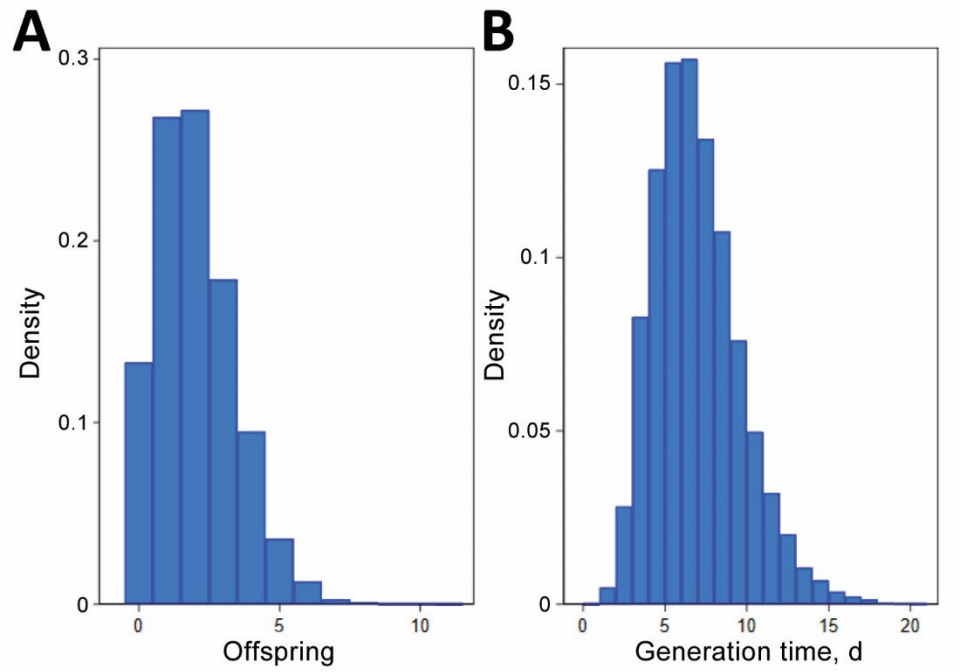

Appendix 1 Figure 1. Offspring (A) and generation time (B) distributions.

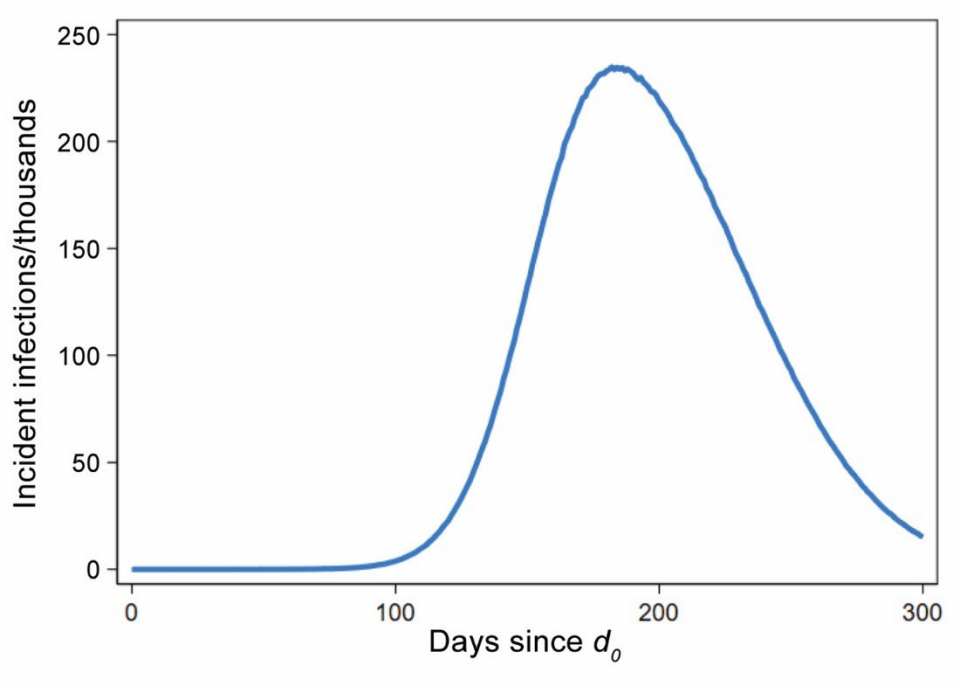

Appendix 1 Figure 2. Simulated epidemic curve at the origin.

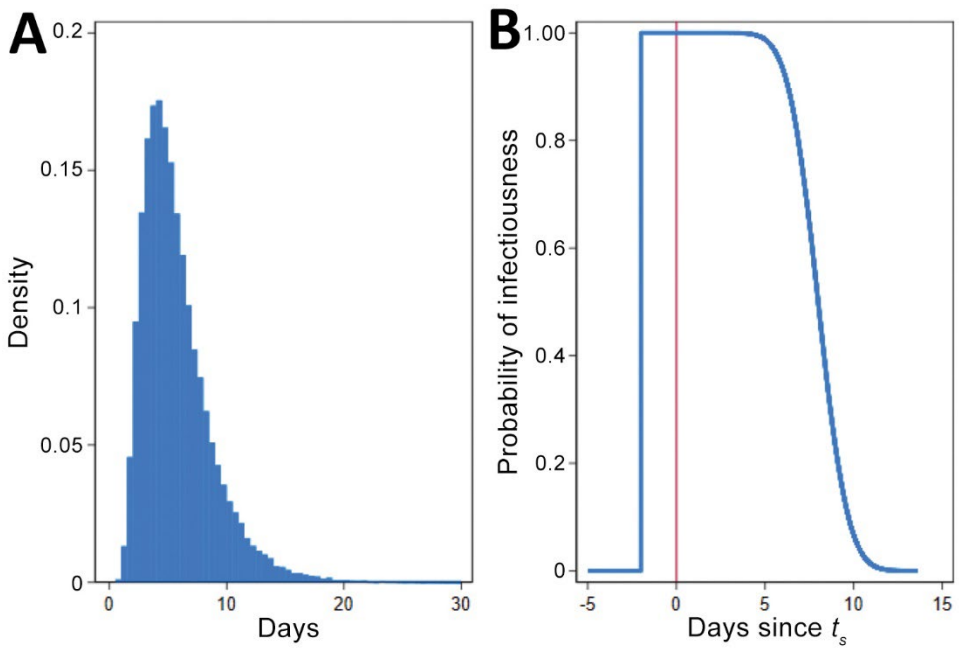

Appendix 1 Figure 3. incubation period distribution (A) and the probability of infectiousness (B).

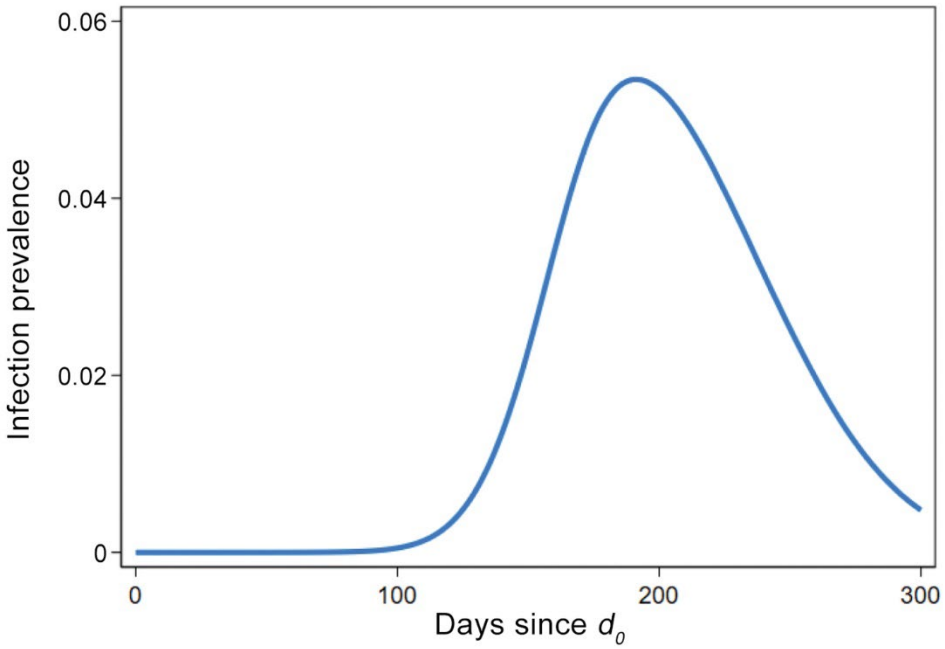

Appendix 1. Figure 4. Simulated infection prevalence at the origin.

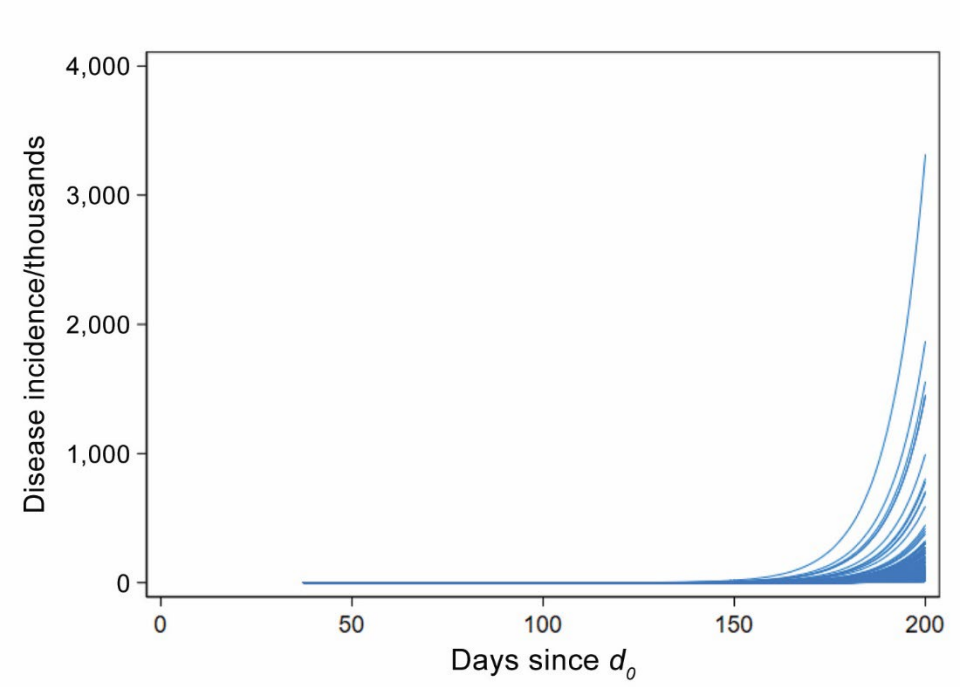

Appendix 1 Figure 5. Simulated disease incidence growth curves within the destination country for 500 arrivals per day by using daily prevalence from Appendix Figure 4.

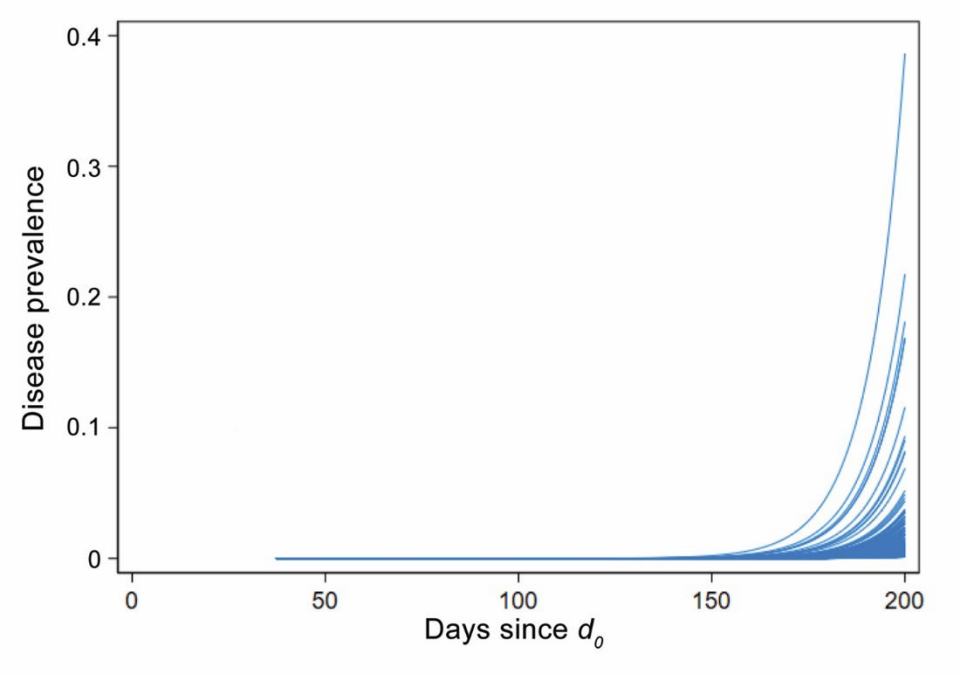

Appendix 1 Figure 6. Simulated disease prevalence growth curves within the destination country for 500 arrivals per day.

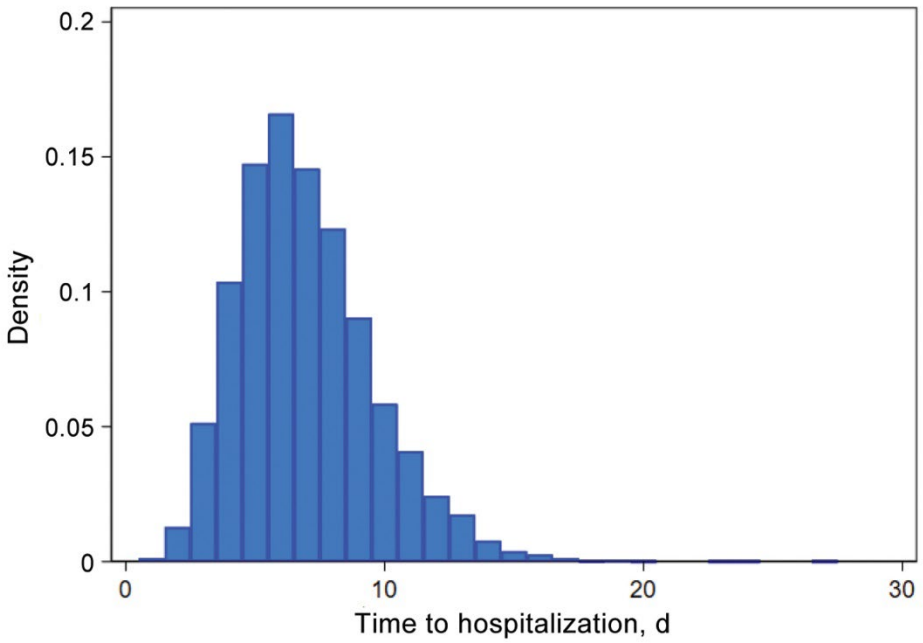

Appendix 1 Figure 7. Time from symptom onset to hospitalization distribution.

Article DOI: https://doi.org/10.3201/eid2911.230492

Simulation Study of Surveillance Strategies for Faster Detection of Novel SARS-CoV-2 Variants

Appendix 2.

Results of Simulations

The 8 tables below provide the results of the simulations described in the main paper and Appendix 1. The nature of simulations means that each time they are run, there will be slight variation in the results produced (not significant enough to change the trends or overall conclusions reported).

Appendix 2 Table 1. Summary statistics for the simulated earliest time to detection distribution for testing at the border with 250 daily passengers, all times refer to days since the index case

Proportion tested	centiles								
	1st	5th	10th	25th	50th	75th	90th	95th	99th
0.010	115	127	136	150	166	184	206	221	253
0.020	106	120	127	140	152	168	181	189	206
0.030	98	112	121	133	146	158	169	174	189
0.040	95	108	118	131	143	154	162	167	178
0.050	91	111	118	128	139	149	157	162	175
0.060	95	107	116	125	137	146	155	161	171
0.070	90	109	116	125	135	144	152	156	164
0.080	94	106	114	124	135	143	151	155	162
0.090	92	106	112	121	131	140	149	153	160
0.100	90	104	109	121	131	140	147	150	157
0.110	89	100	109	120	130	139	146	150	158
0.120	88	101	109	119	128	137	143	147	156
0.130	88	102	108	119	128	136	143	148	153
0.140	86	96	105	116	127	135	141	144	151
0.150	80	99	106	116	126	135	141	145	151
0.160	81	99	105	116	126	134	141	144	151
0.170	84	98	106	115	123	132	140	144	148
0.180	80	97	105	115	124	132	138	142	149
0.190	79	98	106	115	123	132	138	141	147
0.200	85	96	104	114	123	131	137	141	147
0.210	80	97	104	113	123	130	137	140	146
0.220	81	96	102	112	122	129	135	139	145
0.230	78	96	103	111	121	129	135	138	144
0.240	76	92	100	110	120	128	135	138	145
0.250	80	94	100	110	120	128	134	137	143
0.260	82	97	101	110	120	126	133	136	142
0.270	76	95	102	110	119	127	133	137	144
0.280	78	95	101	111	119	126	132	136	142
0.290	73	92	101	109	118	126	132	136	142
0.300	83	94	100	110	119	126	132	136	142

Proportion tested	centiles								
	1st	5th	10th	25th	50th	75th	90th	95th	99th
0.310	76	94	100	109	118	126	131	135	141
0.320	70	90	98	109	117	125	131	134	140
0.330	72	89	97	108	117	125	131	135	140
0.340	77	92	98	106	117	124	130	133	138
0.350	75	89	97	108	116	124	130	134	139
0.360	72	91	98	107	116	124	129	133	140
0.370	65	90	97	106	115	123	130	133	137
0.380	78	91	97	107	116	124	129	133	138
0.390	66	91	97	106	115	122	129	132	138
0.400	78	89	96	107	115	123	128	131	138
0.410	78	90	97	105	115	123	128	131	138
0.420	76	90	97	106	115	122	128	131	136
0.430	74	86	96	107	115	122	128	131	137
0.440	77	90	98	107	115	122	128	130	135
0.450	65	87	95	106	115	122	127	132	138
0.460	68	88	94	105	114	121	126	129	136
0.470	75	90	96	105	113	120	127	129	135
0.480	78	90	96	104	113	120	126	130	135
0.490	73	88	95	105	114	121	126	129	134
0.500	72	86	94	105	114	121	126	130	134

Appendix 2 Table 2. Summary statistics for the simulated earliest time to detection distribution for testing at hospitals with seedings from 250 daily passengers

IHR	Proportion tested	centiles								
		1st	5th	10th	25th	50th	75th	90th	95th	99th
0.005	0.10	128	143	150	161	171	178	185	188	195
0.005	0.20	119	139	145	155	164	173	179	181	187
0.005	0.30	114	134	140	151	161	168	175	178	183
0.005	0.40	116	132	140	150	159	166	172	175	181
0.005	0.50	117	128	137	146	156	164	169	173	179
0.010	0.10	123	137	144	155	165	172	178	182	187
0.010	0.20	115	131	137	147	157	165	172	175	181
0.010	0.30	115	129	136	145	154	162	169	172	178
0.010	0.40	108	124	131	141	151	159	165	168	173
0.010	0.50	107	124	132	141	150	157	164	167	170
0.015	0.10	112	133	139	151	161	168	174	178	183
0.015	0.20	108	125	133	144	155	162	169	172	177
0.015	0.30	101	122	129	142	152	159	165	168	174
0.015	0.40	104	120	128	139	147	156	162	165	169
0.015	0.50	108	122	128	138	147	154	159	162	167
0.020	0.10	115	132	138	149	158	166	171	174	181
0.020	0.20	108	123	131	142	152	160	166	168	174
0.020	0.30	110	123	128	138	148	156	161	165	172
0.020	0.40	102	119	126	137	146	154	160	163	166
0.020	0.50	103	117	124	134	143	151	156	159	164
0.025	0.10	111	128	135	147	156	163	169	173	177
0.025	0.20	108	122	129	140	149	157	162	166	172
0.025	0.30	104	118	127	138	147	154	159	162	168
0.025	0.40	104	119	125	135	143	151	157	159	164
0.025	0.50	104	115	122	132	142	149	155	159	163

Appendix 2 Table 3. Summary statistics for the simulated earliest time to detection distribution for testing at the border with 500 daily passengers, all times refer to days since the index case

Proportion	centiles								
tested	1st	5th	10th	25th	50th	75th	90th	95th	99th
0.010	108	124	130	142	154	167	179	186	207
0.020	103	114	122	131	143	153	163	170	181
0.030	94	109	116	127	138	147	156	160	172
0.040	93	106	112	122	135	144	152	156	163
0.050	89	103	111	122	131	140	147	151	161
0.060	87	102	109	118	129	136	143	146	155
0.070	88	100	108	118	127	136	142	146	154
0.080	79	98	106	116	125	133	140	143	149
0.090	84	97	104	114	124	132	138	142	147
0.100	82	96	103	114	124	132	137	140	147
0.110	81	95	103	112	122	130	136	140	146
0.120	79	94	103	112	121	129	136	138	143
0.130	75	93	102	111	120	128	133	137	143
0.140	77	93	100	110	119	127	133	137	140
0.150	79	93	99	109	118	126	132	135	140
0.160	75	92	98	108	118	125	132	136	140
0.170	79	93	99	109	118	125	131	134	140
0.180	73	89	97	108	116	124	130	133	138
0.190	73	88	97	107	115	123	129	133	138
0.200	76	91	97	105	114	122	127	131	137
0.210	79	90	97	106	115	123	129	131	137
0.220	74	92	97	106	114	121	127	130	137
0.230	76	89	96	106	114	121	127	130	136
0.240	72	87	93	104	113	121	126	130	134
0.250	73	88	97	105	113	120	126	129	135
0.260	68	89	95	105	113	120	126	129	133
0.270	71	87	93	103	112	119	125	127	132
0.280	70	87	95	104	112	119	124	128	134
0.290	64	85	92	101	111	119	125	128	133
0.300	65	83	91	102	111	118	125	127	132
0.310	70	85	92	103	111	118	123	126	131
0.320	70	86	92	102	111	117	123	125	130
0.330	68	86	92	101	110	117	124	127	131
0.340	71	84	90	101	110	117	123	126	131
0.350	71	87	93	101	111	117	123	125	131
0.360	69	86	92	100	109	116	121	125	130
0.370	68	84	91	101	109	116	122	125	129
0.380	68	84	92	100	109	116	121	124	127
0.390	68	84	89	101	109	116	120	123	128
0.400	71	84	90	100	109	116	121	123	128
0.410	65	84	90	100	108	115	120	123	127
0.420	71	86	91	100	107	114	120	122	127
0.430	72	84	90	99	108	115	121	123	128
0.440	69	82	88	98	108	115	120	123	129
0.450	68	82	88	99	107	114	119	122	127
0.460	65	81	88	98	107	115	120	123	128
0.470	56	82	87	98	106	114	119	122	127
0.480	61	83	89	98	106	113	118	121	127
0.490	63	81	88	98	106	113	119	121	125
0.500	63	79	87	97	106	113	118	121	127

Appendix 2 Table 4. Summary statistics for the simulated earliest time to detection distribution for testing at hospitals with seedings from 500 daily passengers

IHR	Proportion tested	centiles								
		1st	5th	10th	25th	50th	75th	90th	95th	99th
0.005	0.10	115	135	143	154	163	171	177	179	184
0.005	0.20	114	128	135	147	156	164	169	172	178
0.005	0.30	117	127	133	144	153	161	167	169	173
0.005	0.40	108	122	131	141	149	157	163	166	172
0.005	0.50	109	121	130	140	148	156	161	164	169
0.010	0.10	121	132	138	147	156	164	170	174	177
0.010	0.20	109	123	128	140	149	157	163	167	172
0.010	0.30	104	121	128	137	147	154	160	163	167
0.010	0.40	105	119	125	135	144	151	157	160	167
0.010	0.50	98	116	123	134	142	149	155	158	163
0.015	0.10	110	128	133	144	153	160	165	168	172
0.015	0.20	104	120	126	137	147	154	160	162	169
0.015	0.30	103	118	125	134	143	151	156	159	164
0.015	0.40	100	112	121	132	141	148	154	157	162
0.015	0.50	95	112	119	130	139	145	151	154	158
0.020	0.10	107	122	130	140	150	158	163	166	172
0.020	0.20	106	118	125	135	144	152	157	161	166
0.020	0.30	101	115	121	132	141	148	153	156	163
0.020	0.40	104	114	119	129	139	146	151	154	159
0.020	0.50	96	111	117	127	136	143	149	151	158
0.025	0.10	107	121	130	139	148	155	162	164	169
0.025	0.20	105	116	123	133	143	150	155	158	162
0.025	0.30	95	114	120	130	138	146	151	154	159
0.025	0.40	94	111	117	127	137	143	149	152	157
0.025	0.50	96	108	115	125	134	141	147	150	154

Appendix 2 Table 5. Summary statistics for the simulated earliest time to detection distribution for testing in community surveillance with seedings from 500 daily passengers

Community survey size	centiles								
	1st	5th	10th	25th	50th	75th	90th	95th	99th
20000	125	139	147	157	166	174	179	183	189
30000	122	137	144	153	163	171	177	180	184
40000	124	134	141	152	161	167	173	176	181
50000	118	132	139	148	158	166	171	173	180
60000	117	131	137	147	157	164	170	173	178
70000	114	127	134	145	155	162	168	171	178
80000	115	128	135	144	154	161	167	170	176
90000	113	126	133	144	153	161	166	169	173
100000	112	128	133	144	152	160	165	168	173
110000	107	126	131	142	152	158	164	167	172
120000	106	123	130	140	150	158	163	167	172
130000	107	123	131	141	150	157	164	167	171
140000	109	124	130	139	148	156	162	164	169
150000	106	122	129	139	148	156	161	164	170
160000	107	120	128	139	148	155	160	164	169
170000	107	121	128	138	148	155	161	163	169
180000	108	119	125	136	146	155	161	164	169
190000	106	121	128	137	146	154	159	162	169
200000	101	119	126	138	146	153	158	161	166

Appendix 2 Table 6. Summary statistics for the simulated earliest time to detection distribution for testing at the border with 100 daily passengers, all times refer to days since the index case

Proportion	centiles								
tested	1st	5th	10th	25th	50th	75th	90th	95th	99th
0.010	118	135	143	159	180	>200	>200	>200	>200
0.020	111	131	140	152	170	189	>200	>200	>200
0.030	103	127	134	148	163	179	196	>200	>200
0.040	108	123	129	142	156	171	186	195	>200
0.050	105	118	126	139	153	165	179	188	>200
0.060	103	117	125	137	150	163	174	182	199
0.070	96	114	122	135	149	161	172	178	191
0.080	97	114	121	134	146	156	167	172	186
0.090	102	115	122	132	144	156	166	172	184
0.100	101	115	122	132	144	154	163	169	180
0.110	98	112	119	130	141	151	161	167	177
0.120	95	112	117	128	140	150	159	164	174
0.130	91	109	116	127	139	148	157	164	172
0.140	97	111	118	128	138	148	157	161	168
0.150	91	110	117	127	137	146	155	161	169
0.160	91	105	114	126	137	146	154	159	168
0.170	97	110	114	125	135	144	153	158	167
0.180	89	105	114	125	134	143	152	157	164
0.190	91	105	114	124	134	143	151	156	164
0.200	87	104	112	123	133	142	150	154	162
0.210	90	103	112	122	132	142	149	155	161
0.220	89	105	111	122	132	141	148	151	158
0.230	88	104	111	122	133	141	148	153	159
0.240	91	104	110	120	132	141	147	152	159
0.250	88	103	110	120	131	140	148	151	157
0.260	83	103	110	121	131	140	146	150	158
0.270	87	103	110	120	130	139	145	150	156
0.280	80	102	111	120	130	138	144	149	154
0.290	86	101	108	119	129	137	144	148	155
0.300	83	100	107	118	128	137	143	148	156
0.310	90	102	110	119	129	137	143	147	153
0.320	87	103	110	118	128	136	143	147	152
0.330	85	101	108	118	127	136	143	146	154
0.340	88	100	108	117	127	136	142	146	154
0.350	83	101	106	116	126	135	141	146	153
0.360	78	100	107	116	126	135	142	145	152
0.370	85	100	107	117	127	135	141	145	153
0.380	82	97	106	116	126	134	141	145	150
0.390	83	97	104	116	125	134	140	144	152
0.400	78	99	106	116	125	133	139	143	150
0.410	78	98	104	115	125	133	140	143	149
0.420	82	99	106	116	125	133	139	144	151
0.430	82	100	106	116	124	133	138	142	148
0.440	77	100	106	115	124	132	139	142	149
0.450	80	97	104	114	124	133	138	142	148
0.460	81	95	103	115	124	131	138	141	148
0.470	87	98	104	114	124	131	138	141	147
0.480	80	97	105	114	123	131	138	141	146
0.490	84	97	104	113	123	131	137	141	149
0.500	84	98	104	113	123	131	136	140	148

Appendix 2 Table 7. Summary statistics for the simulated earliest time to detection distribution for testing at hospitals with seedings from 100 daily passengers

IHR	Proportion tested	centiles								
		1st	5th	10th	25th	50th	75th	90th	95th	99th
0.005	0.10	135	151	159	170	180	189	196	199	>200
0.005	0.20	125	146	153	164	174	182	188	192	198
0.005	0.30	126	141	149	161	171	179	186	189	194
0.005	0.40	120	139	146	158	167	175	182	186	192
0.005	0.50	118	138	144	156	166	174	180	183	188
0.010	0.10	128	146	152	163	173	183	189	192	197
0.010	0.20	128	140	147	157	167	176	182	186	190
0.010	0.30	120	136	143	153	164	172	178	182	188
0.010	0.40	116	134	141	151	161	169	176	180	186
0.010	0.50	114	132	140	151	160	168	175	178	184
0.015	0.10	126	141	147	159	170	178	185	189	195
0.015	0.20	118	135	143	154	164	173	179	182	187
0.015	0.30	113	133	140	151	161	169	175	178	185
0.015	0.40	112	130	136	147	157	165	173	176	182
0.015	0.50	111	130	136	147	156	164	171	174	180
0.020	0.10	123	139	147	157	167	176	183	186	193
0.020	0.20	118	132	141	151	162	170	176	180	186
0.020	0.30	110	129	136	148	157	166	172	176	182
0.020	0.40	113	127	134	145	155	164	170	173	179
0.020	0.50	106	127	134	144	154	161	168	171	177
0.025	0.10	121	136	144	156	165	173	180	183	189
0.025	0.20	114	131	138	149	159	167	174	177	182
0.025	0.30	114	129	136	146	156	164	171	174	179
0.025	0.40	110	126	133	144	153	162	168	171	175
0.025	0.50	110	124	131	142	151	159	165	169	173

Appendix 2 Table 8. Summary statistics for the simulated earliest time to detection distribution for testing in community surveillance with seedings from 100 daily passengers

Community survey size	Centiles								
	1st	5th	10th	25th	50th	75th	90th	95th	99th
20000	139	156	164	175	185	193	200	>200	>200
30000	132	150	158	170	180	189	195	199	>200
40000	136	151	157	168	178	187	193	197	>200
50000	128	144	154	165	176	184	191	196	>200
60000	129	147	153	164	174	183	190	193	198
70000	124	144	150	163	173	181	189	192	198
80000	125	144	150	162	172	180	186	190	196
90000	122	141	149	160	171	179	185	189	194
100000	128	142	149	159	169	177	184	187	194
110000	123	138	147	158	169	177	183	186	192
120000	123	138	147	158	168	176	183	186	192
130000	125	140	147	157	167	175	182	185	190
140000	124	141	148	158	167	175	182	185	191
150000	121	136	144	156	165	174	180	184	191
160000	119	138	146	156	165	174	180	184	189
170000	116	135	143	153	164	172	179	182	188
180000	118	136	143	154	164	173	178	182	188
190000	118	135	143	154	164	172	177	181	188
200000	117	134	142	153	163	171	178	181	187